

Predicting the microbial exposure risks in urban floods using GIS, building simulation, and microbial models

Jonathon Taylor^{1,2}, Phillip Biddulph¹, Michael Davies¹, Ka man Lai²

¹The Bartlett School of Graduate Studies, UCL, London

²Department of Civil, Environmental, and Geomatic Engineering, UCL, London

Abstract

London is expected to experience more frequent periods of intense rainfall and tidal surges, leading to an increase in the risk of flooding. Damp and flooded dwellings can support microbial growth, including mould, bacteria, and protozoa, as well as persistence of flood-borne microorganisms. The amount of time flooded dwellings remain damp will depend on the duration and height of the flood, the contents of the flood water, the drying conditions, and the building construction, leading to particular properties and property types being prone to lingering damp and human pathogen growth or persistence. The impact of flooding on buildings can be simulated using Heat Air and Moisture (HAM) models of varying complexity in order to understand how water can be absorbed and dry out of the building structure. This paper describes the simulation of the drying of building archetypes representative of the English building stock using the EnergyPlus based tool 'UCL-HAMT' in order to determine the drying rates of different abandoned structures flooded to different heights and during different seasons. The results are mapped out using GIS in order to estimate the spatial risk across London in terms of comparative flood vulnerability, as well as for specific flood events. Areas of South and East London were found to be particularly vulnerable to long-term microbial exposure following major flood events.

1. Introduction

London is one of the most flood-vulnerable major cities in Europe, with risks of tidal flooding from the Thames and fluvial and surface water floods from heavy precipitation. Major tidal floods in 1928 and 1953 caused significant damage to the city, while more recently the summer floods of 2007 saw 1,000 London households flooded following heavy rainfall. It has been estimated that a 1 in 50 year rainfall event would lead to the flooding of 1 in 7 London buildings and damages of tens of billions of pounds [GLA, 2009]. In addition, small, localised floods caused by broken water mains are also a regular occurrence. Climate change is projected to result in rising sea levels and an increased frequency of rain storms, which may lead to a greater frequency of flood events in London.

Flooding can lead to a number of health issues for building occupants. Mould, bacteria, and protozoa can grow or persist on flooded building surfaces, some of which can release harmful bioaerosols into the indoor air [Taylor et al., 2011], leading to potential respiratory problems. Building dampness is one of the key factors associated with the exposure to various microbial hazards. Microbial contaminants on indoor surfaces following flooding may also pose a

1 health risk to occupants through direct contact, should they touch a surface that is
2 contaminated with a flood borne pathogen. Occupants who choose to leave their flooded
3 properties because of the risks present in damp properties may also experience increased
4 health problems such as mental illnesses [Tapsell and Tunstall, 2008] related to their
5 displacement. The duration of displacement may be prolonged following a flood; the 2007
6 floods in Hull resulted in over 10% of households remaining in temporary accommodation
7 two years after the event [Hull City Council, 2009]. The reasons for extended displacement
8 can be complex, and include delays in remediation due to insurance issues, busy remediation
9 companies, and the extent of the work required to return the dwelling to a habitable state.
10 However, the amount of time taken to dry different buildings is one of the key issues effecting
11 displacement. Therefore, understanding the duration of damp within buildings under different
12 drying scenarios can help to predict the potential risk to occupants following a flood.

13 Heat, Air, and Moisture (HAM) models are tools used in building simulation to predict
14 moisture performance, from individual materials, to building envelopes and whole-buildings.
15 HAM models have been used in the past for simulating the impact of flooding on buildings.
16 [Blades et al., 2004; Nicolai and Grunewald, 2006; EU, 2007]. In our previous study,
17 simulations of a the drying behaviour of a number of typical London dwellings indicated that
18 there are differences in the drying rates of different dwelling types following a flood due to
19 the built form and building fabric construction and drying type [Taylor et al, 2012]. One of
20 the key findings of this research was that modern purpose-built flats were more difficult to
21 dry then detached or semi-detached properties, and that buildings with cavity walls insulated
22 with glass fibre, or with an Autoclaved Aerated Concrete (AAC) inner leaf were more
23 difficult to dry than those with solid brick or uninsulated cavity walls with a brick inner leaf.

24 The types of dwellings and their building fabrics vary throughout London, meaning that the
25 results from our previous research can be applied spatially to determine the drying difficulty
26 of different locations within the research area. Similarly, the depth of flood water during flood
27 events will also vary spatially, meaning that simulations that take into account the depth of a
28 flood event may be applied to models of specific floods in order to predict areas of
29 vulnerability within London. Finally, the city population varies spatially in terms of its socio-
30 demographic profile and population density, and therefore it's vulnerability to health problems
31 following a flood event.

32 The objective of this paper is to integrate the results of HAM building simulations with GIS-
33 based building stock models and flood models in order to predict the locations within London
34 that are particularly vulnerable to long-term damp following a flood event. Building on
35 previous research, the drying behaviour of different London archetypical buildings will be
36 simulated drying under different conditions and after floods of different heights. The mould
37 model of Clarke et al [Clarke, 1998] is used to predict the risk of mould growth on different
38 surfaces within the flooded buildings and determine the total internal surface area presenting
39 a microbial risk. The simulation results will be used to map both the comparative drying
40 ability of the buildings in different locations by examining the drying time under the same
41 flooding and drying conditions, and the actual drying behaviour after a specific flood event by
42 taking the flood height into account for individual buildings. Finally, areas which may be at
43 high risk due to a high risk of floods, an abundance of slow drying buildings, social
44 vulnerability, and population density are identified. The results of this analysis can be used to
45 identify areas where the city may be particularly vulnerable to the effects of flooding due to
46 the combination of built form, demographics, and flood risk.

48 **2. Methodology**

49
50 This research required combining a number of different data sources and models including
51 building stock models, HAM simulations, GIS data, and flood models. For more information

1 on the building stock development, HAM models used, and modelling methodology, readers
2 are advised to refer to Taylor et al [2012].
3

4 **2.1 Building Simulation**

5
6

7 The building stock archetypes used in this study were originally developed by Oikonomou
8 [Oikonomou et al., 2011] and represent 15 of the most commonly occurring built form and
9 dwelling age combinations within their research area (29% of the Greater London Authority
10 household spaces). Some dwellings were not relevant, for example flats above ground level
11 and those with shops underneath, as they would not be directly impacted by flood waters.
12 The English Housing Survey [DCLG, 2008] was used to identify the most common building
13 fabric types in each building archetype; in cases of cavity walls, both insulated and
14 uninsulated walls were considered. Hygrothermal material data for the construction materials
15 in the building envelopes were taken from the WUFI database [IBP, 2007], while information
16 on glass fibre was taken from Hokoi and Kumaran (1993).
17

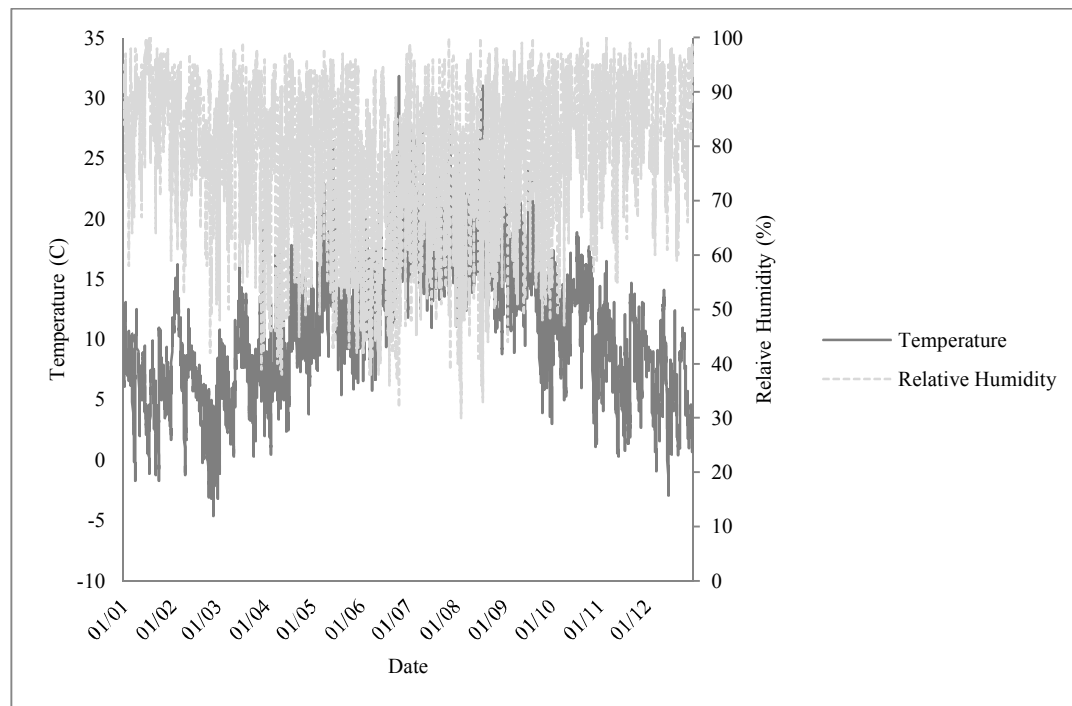
18 The methodology for simulating the flooding and drying of the archetypes using HAM
19 models has been previously described in Taylor et al [2012]; this paper expands on this initial
20 work by simulating floods at a number of different flood heights. No simulation package was
21 known to be available that would allow both the simulation of water movement into a
22 structure using a pressure head of water, and the whole-building simulation of the internal and
23 external drying of the building. Therefore, two separate HAM models were used to simulate
24 the flooding and drying of the buildings: Delphin 5.6 [Nicolai and Grunewald, 2006] and the
25 EnergyPlus-integrated UCL-HAMT (University College London Heat and Moisture Transfer)
26 [EnergyPlus, 2008]. Delphin was used to simulate the flooding of the wall and floor
27 assemblies, while UCL-HAMT was used to simulate the drying of whole buildings. Two
28 drying scenarios were considered:
29

- 30 • Comparative drying performance: The drying performance of building archetypes
31 under the same drying conditions and flood height were used to illustrate the
32 difficulty of drying property types. In this case, buildings were modelled as being
33 naturally ventilated buildings with their windows and internal doors open and no
34 central heating following a flood of 0.5m on January 1st. Abandoned buildings were
35 modelled with all windows and internal doors closed and the heating turned off. A
36 flood height of 0.5m was selected based on the modelled maximum height of a 1 in
37 20 year tidal flood risk for Hackney, East London
38
- 39 • Actual drying performance: Buildings were simulated as being abandoned, with the
40 windows and external doors closed following a flood on January 1st and July 1st.
41 Buildings were modelled flooded to four different heights (0.1m, 0.5m, 0.7-1.0m, and
42 2.0m) to examine the relationship between flood height and drying time. The range of
43 flood heights (0.7-1.0m) for the second highest flood was due to the presence of
44 internal doors within the building; as the ceiling height varied in the different
45 dwellings, the flood height had to be shifted to accommodate the 2m high door on
46 internal surfaces, and ensuring that the airflow network remained consistent
47 throughout all the flood heights. Buildings were modelled as being abandoned as it
48 was assumed that the flooded homes would be evacuated or sealed following a major
49 flood.
50
51
52
53

1
2 To simplify the model, cavities in the external wall and subfloor were modelled in certain
3 assembly types by including a layer of air or insulation in the HAMT assembly. As a
4 consequence, ventilation within these spaces was not modelled, an assumption which may
5 impact drying behaviour, but is representative of a worst-case scenario where air bricks are
6 blocked or not present.

7
8 External conditions were taken from a CIBSE Test Reference Year weather file for London
9 (Figure 1). The flood simulations were started on January 1st, modelling winter floods on
10 North/South oriented buildings only. The simulation timestep was 1 minute. The RH and
11 temperature were output from the surface cell of the interior side of the walls, floors, and
12 ceilings inside the buildings as an hourly average.

13
14 Simulation duration took from 4-12 hours to simulate a single building on a 2.83GHz Intel
15 processor, depending on the building structure and the complexity of the building fabric. In
16 order to increase the speed of simulation, naïve parallelisation was used to run multiple
17 simulations on a single quad-core computer. Additionally, multiple instances were run on the
18 Amazon Elastic Compute Cloud (EC2), as per Hopkins [Hopkins et al., 2011].



20
21 **Figure 1. Temperature and RH values for the simulation weather file.**

22
23
24
25 The surface relative humidity and temperature were used to calculate the risk of mould
26 growth using the model developed by Clarke [Clarke, 1998] for *Aspergillus versicolor* and *S.*
27 *chartarum* over time. *Apergillus*, and *Stachybotrys* species of fungi have all been observed in
28 elevated levels in flooded dwellings [Solomon et al., 2006; Dumon et al., 2009], but show
29 different moisture requirements with *S. chartarum* having higher moisture requirements than
30 *A. versicolor* for growth. A Microsoft Excel macro was used to automate the import of the
31 EnergyPlus output files and the total surface area of the building susceptible to mould growth
32 was calculated.

2.2 Drying Behaviours

The simulation results were used to demonstrate the drying behaviours of the different building archetypes under comparative and actual drying scenarios.

2.2.1 Comparative Drying Behaviour

The comparative drying behaviour of the buildings was taken to be the amount of time (days) required for the buildings to dry to the point where there was no growth risk for *A. versicolor* or *S. chartarum* on any surface inside the dwellings under naturally ventilated scenarios after the 0.5m winter flood. The same flood height and drying scenario was chosen in order to demonstrate the drying abilities of the archetypes under the same conditions.

2.2.2 Actual Drying Behaviour

Those entering properties for the first time following a major flood event will likely be entering an abandoned property where the doors and windows were left closed to prevent intruders during the evacuation of the occupants. Depth-drying curves were developed to predict the instantaneous mould risk inside the property as well as the amount of time a building will remain at risk following a flood event when left abandoned, based on the height-dependent simulation results. These depth-drying curves are based on the depth-damage curves developed for the prediction of financial costs associated with flooding (e.g. [Penning-Rowse et al., 2005]), and are intended to be applied between the simulated ranges of 0.1m to 2m for different building types and seasons.

In order to describe both the instantaneous risk within a property and the amount of time required for the risk to decrease to zero for *A. versicolor* and *S. chartarum*, a 3D function was fit to the simulation results for the data in the simulated ranges of 0.1m to 2.0m for different building types and seasons. A 3D logistic decline model describes a curve showing the reduction in surface area at risk to mould growth as observed in the simulation results:

$$SA = \frac{a}{1 + \exp(-(b + c * t + d * h + f * t * h))} + g$$

where SA is the internal surface area at risk of mould growth (m²), h is flood height (m), t is time (days), and a, b, c, d, f, and g are model parameters. The logistic equation could be re-arranged in order to solve for the amount of time required for the internal surface areas inside the dwellings to reduce to a set value for floods as a function of flood height:

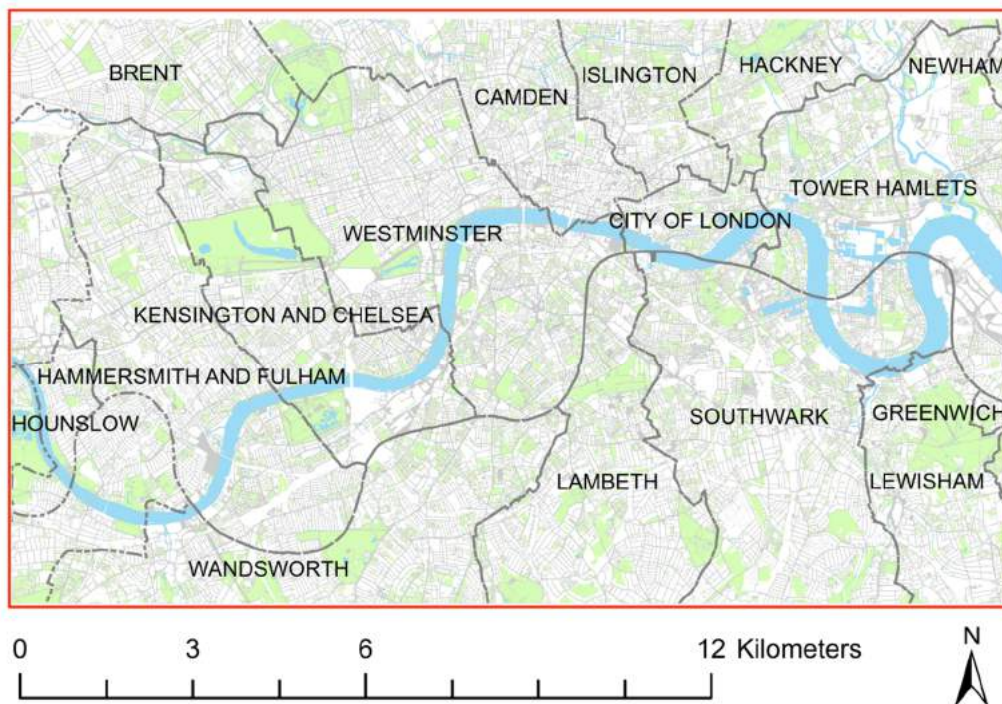
$$t = \frac{\ln\left(\frac{a}{-g} - 1\right) + b + d * h}{c + f * h}$$

This logistic model displays an asymptote which approaches zero over time. In order to force the model to go through SA = 0 when there was no longer a risk of mould growth, the models were fit using a fixed offset (g) set to a nominal value below zero (-10). A major strength of the 3D logistic model is the ability to alter the shape of the decline (concave vs convex decline) by eliminating a model parameter, and making the model applicable to the declines exhibited by both mould species as the buildings dried over time.

1 The data was fit to the curve using the online tool ZunZun [ZunZun.com, 2011], fitting to the
2 lowest sum of squared (SSQ) absolute error. A step-wise regression procedure was followed
3 to eliminate parameters with a large confidence interval. The results were checked against the
4 original data to ensure that the estimate for the drying time (zero- intercept) provided a good
5 estimate of the model results. The parameters for the depth drying curves were calculated for
6 each built form/wall type combination, including both uninsulated and insulated cavity walls
7 in some dwelling types.
8

9 2.3 GIS

10
11 The research area for the present study was selected to be an area of London extending from
12 Richmond in the west to Greenwich in the east – an area covered by approximately 250,000
13 homes, and at risk of flooding (Figure 2). The extent of the research area was determined by
14 the available building stock and surface height data, and computing power.

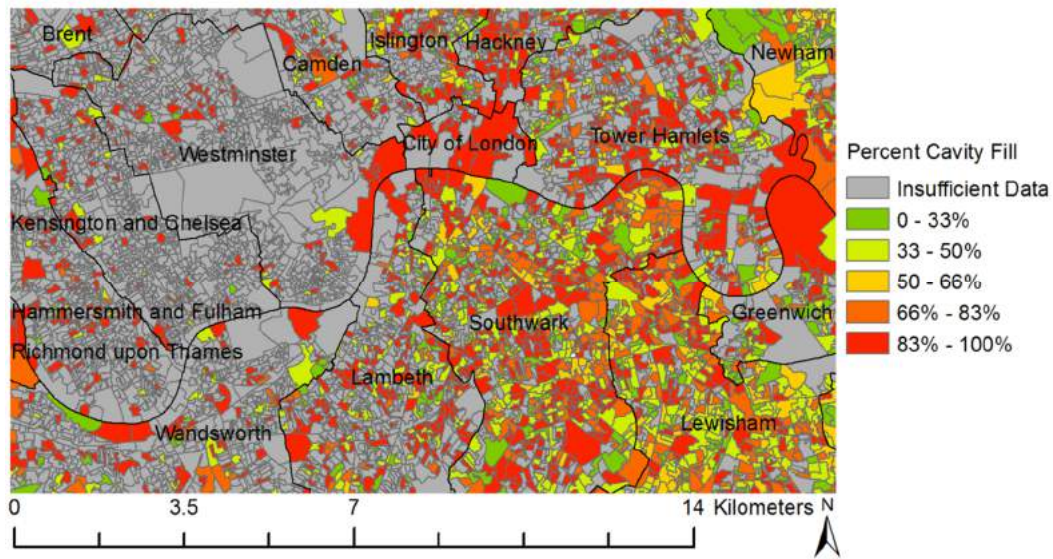


15
16 **Figure 2. Extent of the research area.**

17
18 Cities Revealed (CR) [The Geoinformation Group, 2010] and the Ordnance Survey (OS)
19 [Ordnance Survey, 2010] both produce cadastral maps that were used in this research. CR
20 produces a landuse database with building footprints classified as one of 15 building types
21 and 17 age categories, enabling the archetypes proposed above to be mapped to individual
22 properties within the GIS system. The CR geographic dataset is less frequently updated, less
23 widely available, and a less clear provenance than that of the OS Mastermap. For this reason,
24 the OS Mastermap was used as the basis for the cadastral map of the buildings within the
25 research area.

26
27 CR building classifications were joined to the OS data through a spatial join, so that the
28 individual OS buildings would be matched with the corresponding CR building information
29 based on the location. The resulting cadastral database was filtered for domestic dwellings by
30 based on the CR land use classifications of different properties.
31

1 While the EHCS analysis described the frequency of different wall types within building
2 archetypes, the frequency of cavity wall insulation in archetypes with cavity walls is expected
3 to change depending of the locations of the buildings due to regional differences in income
4 and local government programs. The HEED database [HEED, 2009] is a collection of
5 information from energy suppliers, government scheme managers, local landlords, Energy
6 Saving Trust (EST) energy checks, and EST programmes on wall types, cavity wall insulation
7 levels, and building ages. The HEED database was used to gather additional information
8 about the building fabrics of the buildings within the CR database. COA-level data on the
9 percentage of properties with cavity wall insulation was used to determine the probability of a
10 building with cavity walls having insulation within these areas using the ArcGIS spatial
11 overlay tool. The calculated frequency of insulation within a COA was used to adjust the
12 modal wall type of individual buildings within the areas to reflect the local insulation rates.
13

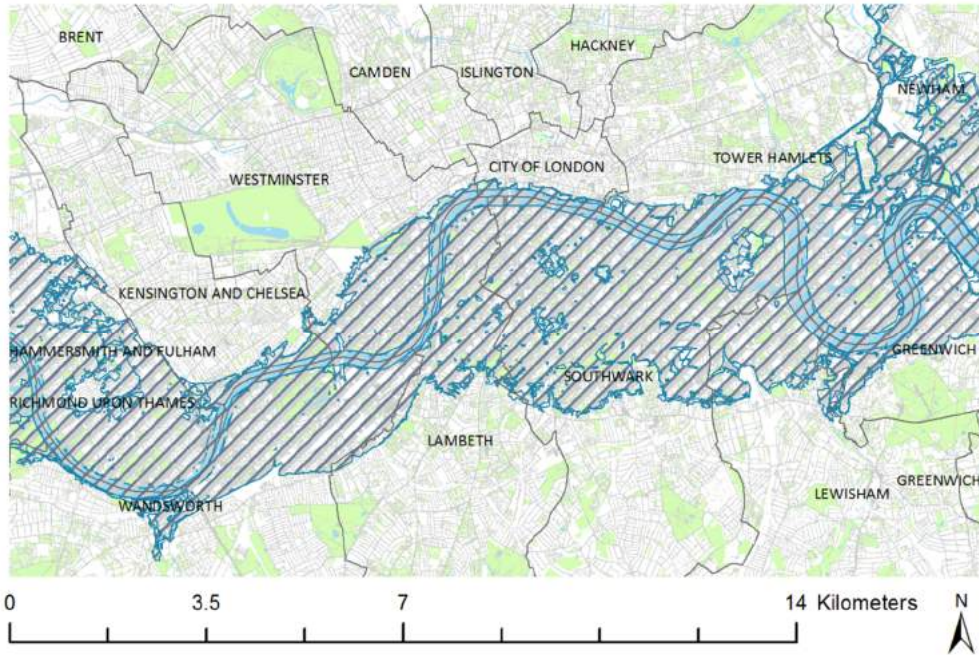


14
15 **Figure 3. The frequency of insulation in cavity walls.**
16

17 **2.3.1 Flood Risk Models**

18 A number of flood risk models are available for the UK, which indicate the risk to certain
19 areas of flooding from different water sources. The Environment Agency (EA) produces
20 publically available flood maps for tidal and fluvial floods [EA, 2010], showing the areas at
21 risk for flood events. A flood map with heights for a 1-in-200 year tidal flood event was
22 obtained from the EA for the research area.

1



2
3

Figure 4. EA 1-in-200 year tidal flood risk map for London.

4

5

6

7

8

9

10

11

12

13

14

15

16

17

18

19

20

21

22

23

24

25

26

27

In order to determine the flood depth for individual properties, a Digital Terrain Model (DTM) was created developed by filtering a LiDAR -generated Digital Elevation Model (DEM) raster provided by CR to remove buildings and other non-terrain features. To filter buildings from the DEM, the building footprints from the original unfiltered OS Mastermap data were used as a mask; using external data as a mask is an established technique in DEM filtering. A 3m buffer was drawn around the outside of the individual building footprints in order to account for the 2m resolution of the LiDAR data and the area within the buffer clipped from the LiDAR dataset. The DEM was then filtered using a slope-based technique, as per the EA [Priestnall, 2000]. Once the raster had been filtered, the gaps were filled by re-interpolating to a 2m resolution using an Inverse Distance Weighting (IDW) algorithm, leaving a DEM representing the height of the ground without man-made or vegetation features.

In order to determine the flood heights above ground level, the DTM was subtracted from the flood height raster using raster math. The flood height for individual properties was determined using the ArcGIS Zonal Statistics tool. A buffer was drawn 1m inside the OS Mastermap building shapefiles and the ArcGIS Spatial Analyst Zonal Statistics tool used to determine the mean floodwater height within the buffered area, and the results were appended to the building stock dataset. Buildings that had a flood height below the simulated range of 0.1m to 2.0m were approximated to be 0.1m, while those above 2m were assumed to have suffered structural damage, and were not considered in this analysis.

28

2.3.2 Mapping Drying Data

29

30

31

32

33

By simulating dwellings drying after the same flood height, and under the same drying conditions, information of the comparative difficulty to dry of dwellings was obtained, while height related drying information for abandoned dwellings allowed for the actual drying behaviour to be modelled. The comparative drying behaviour of different buildings was

1 mapped to demonstrate the variation in vulnerability of locations within the research area
2 regardless of flood event and depth, while the actual drying behaviour took into account the
3 flood depth as calculated by the flood risk model.
4

5 **2.3.2.1 Comparative Drying Behaviour**

6
7 The comparative drying behaviour was taken to be the length of time following the flood
8 required for the modelled built form/wall type combinations to dry under the same naturally
9 ventilated conditions to the point where there was no mould growth risk inside the dwellings,
10 with the assumption that all visible mould would be removed before the occupants move back
11 in. The drying results were joined to the geodatabase of individual buildings with the CR built
12 form and HEED cavity wall insulation data. The mode drying time was then calculated for
13 each COA in the research area using the ArcGIS Overlay-Spatial join tool, resulting in an
14 estimate of the comparative drying times of the most common building archetypes within the
15 COAs. Maps were created for the comparative drying times of the different contaminating
16 species modelled, and used to identify locations where the building types would be vulnerable
17 to long-term damp following flooding. In cases where the built form/wall type combinations
18 did not dry using natural ventilation within the year-long simulation period, the individual
19 buildings were classified as being > 1 year.
20

21 **2.3.2.2 Actual Drying Rates**

22
23 The parameters of the depth-drying curves were joined to the building stock geodatabase, and
24 the flood depths used to calculate the duration of contaminant risk for *A. versicolor* and *S.*
25 *chartarum* for both summer and winter floods. The mean risk duration for the COAs was
26 calculated using the ArcGIS Overlay-Spatial join tool, and the results mapped.
27

28 **2.3.3 Mapping Populations Demographics and Vulnerability**

29
30 Mapping has also been used to show the vulnerability of resident populations to floods based
31 on socioeconomic data and using research into past flooding events. The Social Flood
32 Vulnerability Index [Tapsell, 2002] assesses the vulnerability of populations to adverse health
33 effects based on three social characteristics and four financial-deprivation indicators. To
34 know which populations are at risk from floods for socioeconomic reasons informs the
35 development of processes to predict regions vulnerable to flooding in London. The UK
36 Census [ONS, 2001] provides aggregate statistics on the demographics and socio-economics
37 of the UK within specific geographic areas. This data is used extensively to determine
38 population characteristics within a region, and can be used to describe a flood-affected
39 population.
40

41 To map the vulnerability of Londoners to a flood event, 2001 Census data was acquired from
42 the Census Dissemination Unit for the four financial indicators (Unemployment,
43 Overcrowding, Non-car ownership, and Non-home ownership) and three social indicators
44 (Long-term sick, Single parents, and the Elderly (over 75)) over a COA. The resultant SFVI
45 was mapped using ArcGIS to the census output area level.
46

47 In addition to the SFVI, Census data was obtained for the number of individuals living in
48 households and the number of households within the COAs. The average actual drying time
49 predicted for each COA for *A. versicolor* and *S. chartarum* for the EA 1-in-200 year tidal
50 flood event was multiplied by the average number of individuals per dwelling within the
51 COA in order to estimate the number of person-years residents would be exposed to damp

1 indoor spaces (should they choose to stay), or displaced (should they leave their damp
 2 homes).
 3

4 **3. Results**

6 **3.1 Simulations**

7 **3.1.1 Comparative Drying Behaviour**

8
 9 Comparative drying times were calculated as being the amount of time taken for the microbial
 10 risk inside buildings drying in winter under natural ventilation conditions to decrease to zero
 11 on all internal surface areas. The drying time for each building archetype with their modal
 12 wall type was calculated for each microbial species modelled (Table 1).
 13

14 **Table 1. Drying time (days) of archetypes using natural ventilation following a 0.5m winter flood.**

Building	Wall	<i>A. versicolor</i>	<i>S. chartarum</i>
H01	Solid Brick Wall & Suspended Wooden Floor	201	180
H02	Uninsulated Brick/Brick Cavity	180	161
	Insulated Brick/Brick Cavity	234	222
H03	Uninsulated Brick/Brick Cavity	162	142
	Insulated Brick/Brick Cavity	219	208
H04	Uninsulated Brick/AAC Cavity	> 365	234
	Insulated Brick/AAC Cavity	> 366	272
H05	Solid Brick Wall & Suspended Wooden Floor	213	186
H06	Uninsulated Brick/Brick Cavity	191	163
	Insulated Brick/Brick Cavity	261	233
H07	Uninsulated Brick/AAC Cavity	> 365	234
	Insulated Brick/AAC Cavity	> 366	272
H08	Solid Brick Wall & Suspended Wooden Floor	216	198
H09	Uninsulated Brick/Brick Cavity	172	150
	Insulated Brick/Brick Cavity	218	201
H10	Uninsulated Brick/AAC Cavity	> 365	162
	Insulated Brick/AAC Cavity	> 366	271
H11	Uninsulated Brick/AAC Cavity	> 367	271
	Insulated Brick/AAC Cavity	> 368	321
H12	Solid Brick Wall	233	216
H14	Uninsulated Brick/Brick Cavity	180	161
	Insulated Brick/Brick Cavity	234	222
H15	Uninsulated Brick/Brick Cavity	218	198
	Insulated Brick/Brick Cavity	272	246

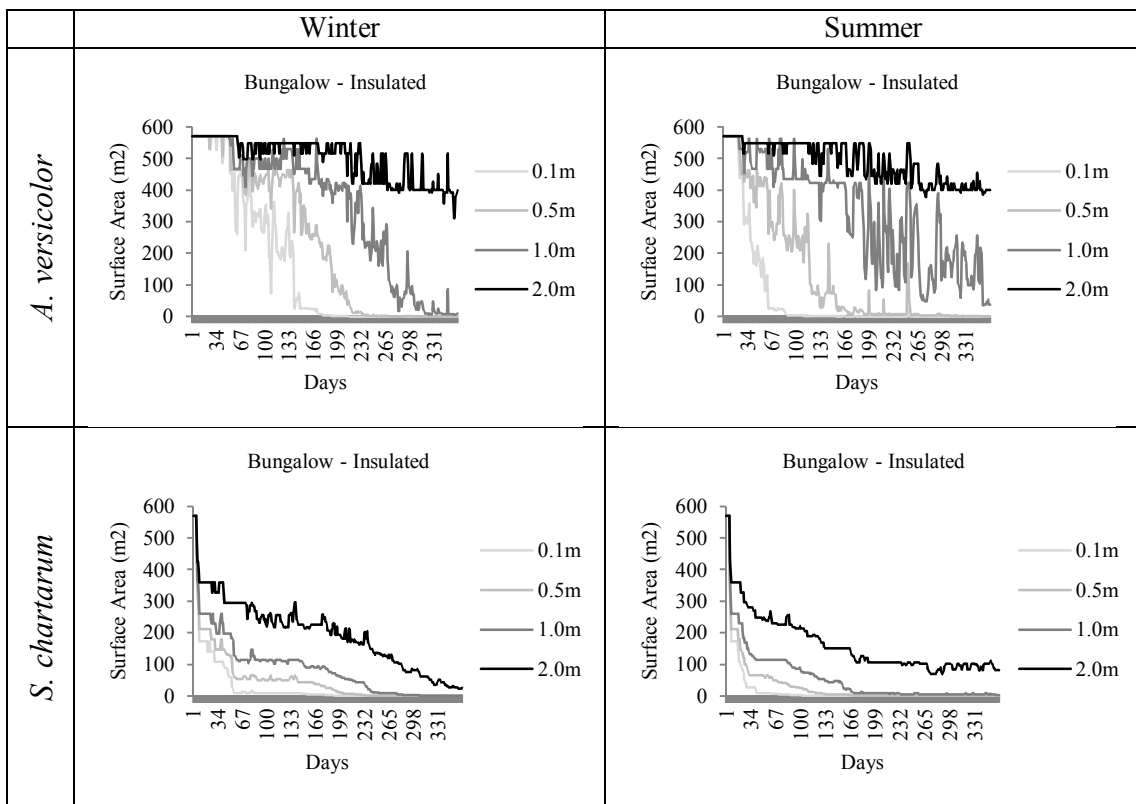
15
 16

17 **3.1.2 Actual Drying Behaviour**

18

1 As expected, dwellings that were flooded to a greater depth took a longer time to dry than the
 2 shallower flood events. The reduced drying rate caused by a lack of ventilation, and the
 3 increased amount of water inside buildings caused by high flood levels meant that many
 4 buildings showed a risk for microbial growth for the entire year-long simulation period. Due
 5 to the moisture requirements of the different species, *A. versicolor* remained a risk inside
 6 buildings for longer than *S. chartarum*.

7
 8 Figure 5 shows the impact of flood height on drying behaviour of a bungalow (Archetype
 9 H09), as well as the differences in the drying rate for abandoned buildings following winter
 10 and a summer flood. Winter floods were found to generally dry slower than summer floods.
 11 Exceptions were observed for buildings that had a wall type that was particularly slow to dry,
 12 such as insulated AAC walls, where the drying period ran into the winter, extending the
 13 amount of time required for the structure to dry.



16 **Figure 5. An example of the drying behaviour of archetype H9 (bungalow) following floods of**
 17 **four different heights for summer and winter floods.**

18
 19 The parameters and model fits for the depth drying curves for each building for *A. versicolor*
 20 contamination risk following a winter flood can be seen in Table 2. The fit of the model is
 21 indicated by the R² and RMSE of the model fit, and the confidence intervals of the parameter
 22 estimates. The models were found to offer a strong estimate of the variation of the drying
 23 rates of buildings flooded to different heights.

24
 25 **Table 2. Parameters for a depth-drying curve for *A. versicolor* growth risk following a winter**
 26 **flood.**

Dwelling	Wall	a	b	c	d	f	g	r-square	RMSE
H01	Pre19299Solid	573	3.3	-0.03	6.32	-	-10	0.955	49.7
H02	Uninsulated	461	3.24	-0.0302	4.53	-	-10	0.941	47.2
	Insulated	465	3.14	-0.029	4.39	-	-10	0.938	48.4

H03	Uninsulated	493	1.73	-0.0239	0.0379	0.00726	-10	0.91	45.8
	Insulated	493	1.73	-0.0239	0.0379	0.00726	-10	0.91	40.8
H04	Uninsulated AAC	271	2.93	-0.00678	2.62	-	-10	0.794	9.9
	Insulated AAC	271	2.93	-0.00678	2.62	-	-10	0.794	9.9
H05	Pre19299Solid	461	3.42	-0.032	7.08	-	-10	0.948	42.2
H06	Uninsulated	234	6.24	-0.0272	3.61	-	-10	0.833	28.6
	Insulated	234	6.24	-0.0272	3.61	-	-10	0.833	29.6
H07	Uninsulated AAC	271	2.93	-0.00678	2.62	-	-10	0.794	9.9
	Insulated AAC	271	2.93	-0.00678	2.62	-	-10	0.794	9.9
H08	Pre19299Solid	633	0.435	-0.0217	5.45	-	-10	0.941	64.6
H09	Uninsulated	520	2.91	-0.0369	5.69	-	-10	0.958	48.3
	Insulated	528	3.16	-0.0335	4.45	0.000716	-10	0.961	44.9
H10	Uninsulated AAC	483	2.93	-0.019	4.56	-	-10	0.879	51.7
	Insulated AAC	483	2.93	-0.019	4.56	-	-10	0.879	51.7
H11	Uninsulated	296	1.42	-0.00893	1.94	-	-10	0.863	27
	Insulated	296	1.42	-0.00893	1.94	-	-10	0.863	27
H12	9InchSolidBrick	281	1.76	-0.0239	5.94	-0.00541	-10	0.957	24.5
H14	Uninsulated	465	3.14	-0.029	4.39	-	-10	0.938	48.4
	Insulated	493	1.73	-0.0239	0.0379	0.00726	-10	0.91	45.8
H15	Uninsulated	296	1.42	-0.00893	1.94	-	-10	0.863	27
	Insulated	296	1.42	-0.00893	1.94	-	-10	0.863	27

1 3.2 GIS

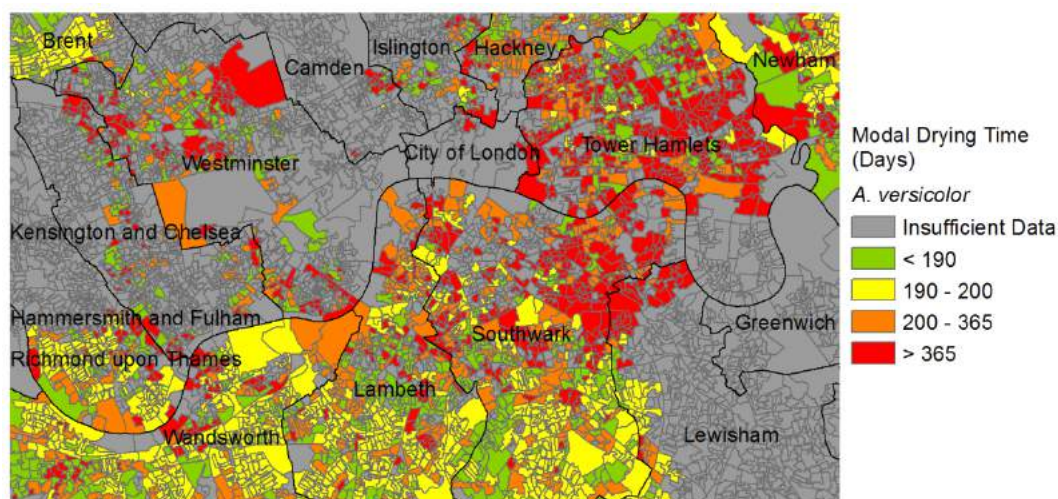
2

3 3.2.1 Comparative Drying Behaviour

4

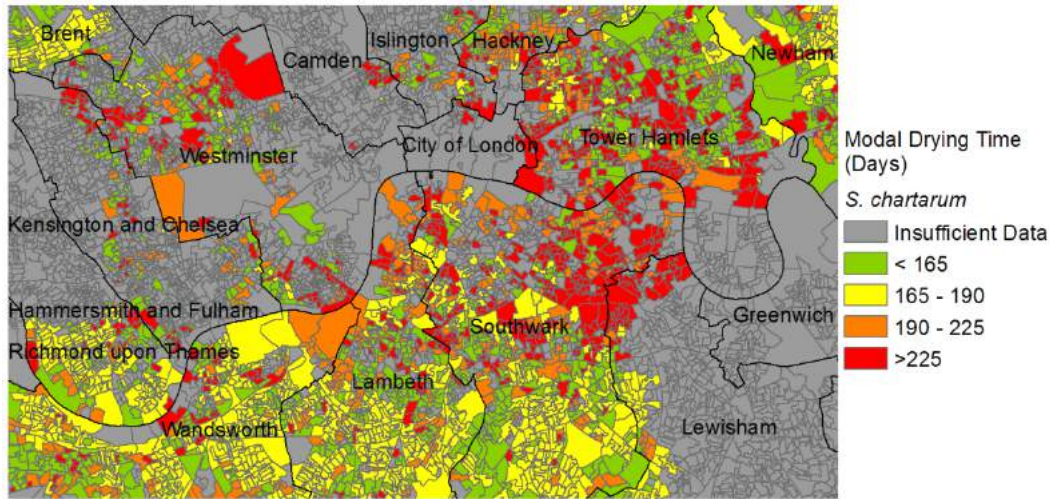
5 The areal mode of the drying times of the building archetypes within London for the different
6 contaminants modelled can be seen in Figure 6 and Figure 7.

7



8

9 **Figure 6. Comparative vulnerability of the London building stock to prolonged *A. versicolor* risk**
10 **following flooding.**

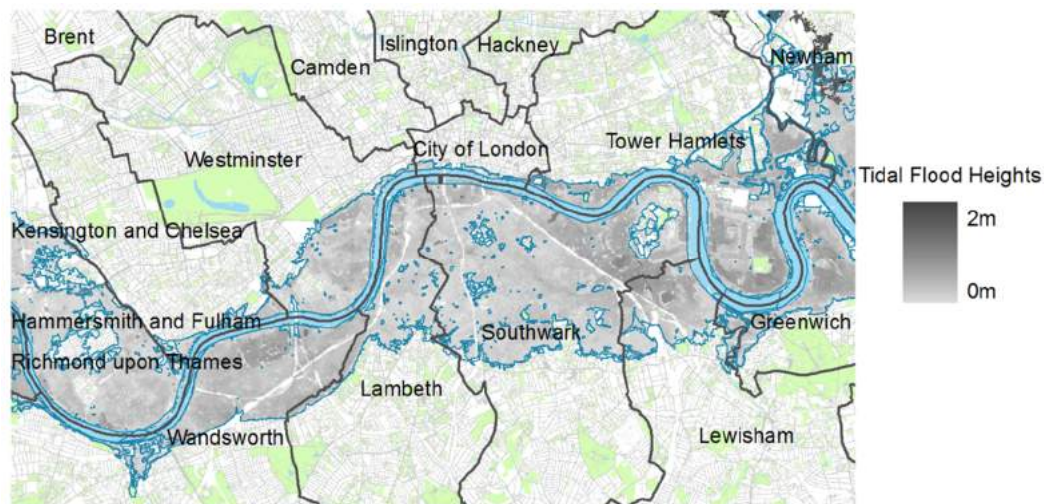


1
2 **Figure 7. Comparative vulnerability of the London building stock to prolonged *S. chartarum* risk**
3 **following flooding.**

4
5 These maps suggest a higher proportion of hard-to-dry properties in the East of the study area.
6 Southwark and Tower Hamlets appear to be particularly vulnerable because of their large
7 number of relatively slow drying properties. There was insufficient data to calculate many of
8 the areas in the study, due to a lack of coverage of the CR data and because the archetypes
9 modelled did not contain all of the London building stock. However, the results give an
10 indication of the drying performance of buildings across many areas of the city.

11 **3.2.2 Actual Drying Behaviour**

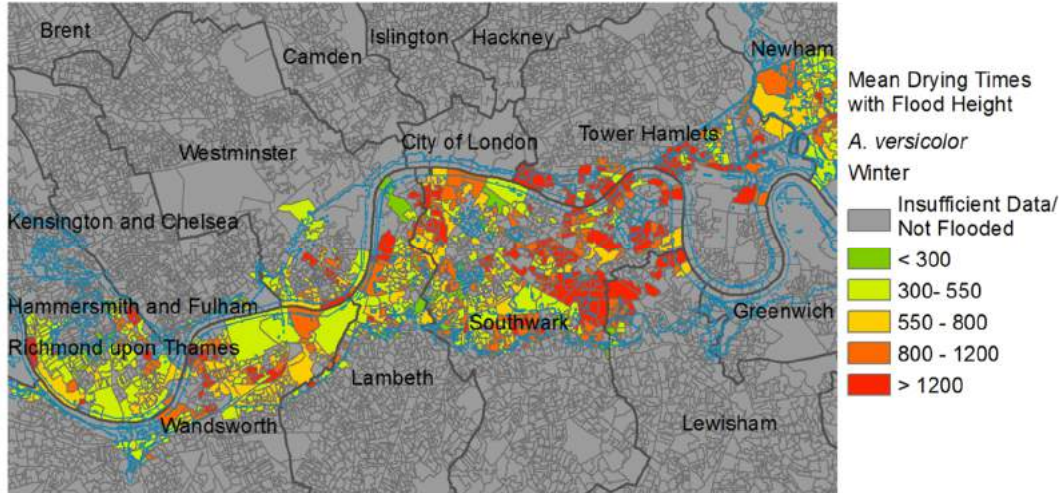
12
13 The raster indicating the calculated depth of the flood event based on the differences between
14 the predicted flood heights provided by the EA and the calculated DTM can be seen in Figure
15 8. The average depth was found to be 0.8m, with parts of Southwark close to the Thames
16 particularly vulnerable to deep flooding based on this scenario. The east of the research area
17 alongside the Thames was found to be vulnerable to particularly deep flooding based on this
18 scenario.



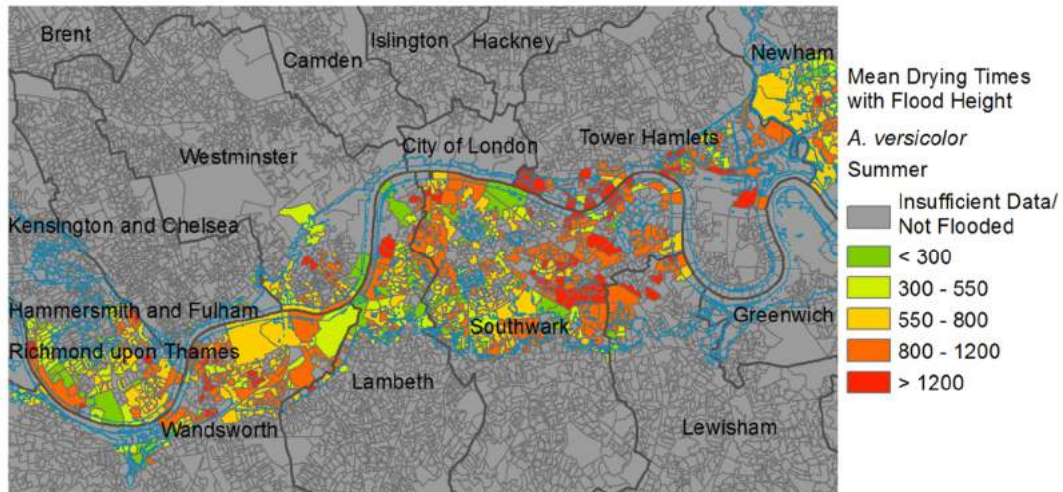
21
22 **Figure 8. The depths of a 1-in-200 year tidal flood event in London.**

23
24 Calculating the mean drying times of all known buildings within the COAs in London
25 allowed for the estimation of how the variation in flood heights may impact on the drying

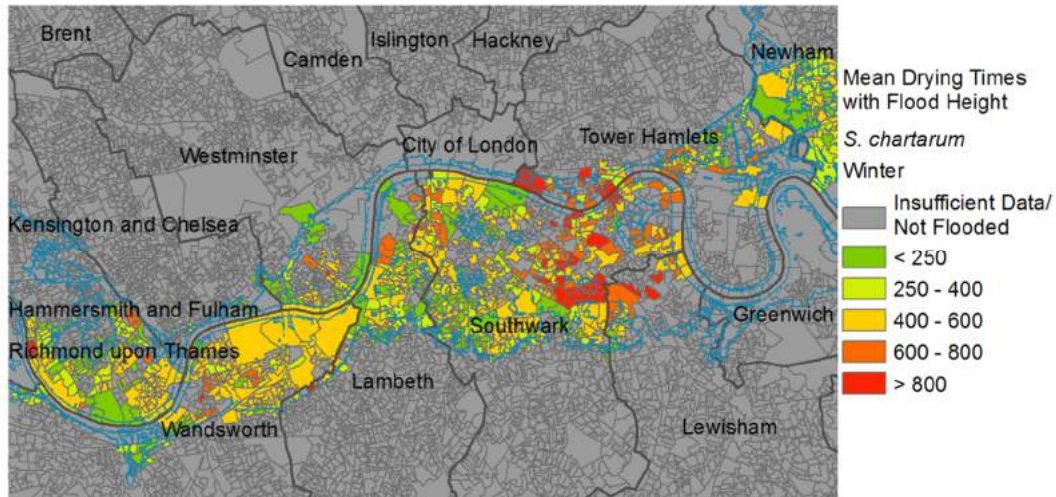
1 rates of properties based on their location. The application of the depth-drying curves to the
 2 tidal flood risk scenario for the mould contaminants following winter and summer floods can
 3 be seen in Figure 9, Figure 10, Figure 11, and Figure 12. As with the comparative drying
 4 results, Southwark was found to be particularly vulnerable to long-term damp, and by taking
 5 into account flood depth, the problem was emphasised.
 6



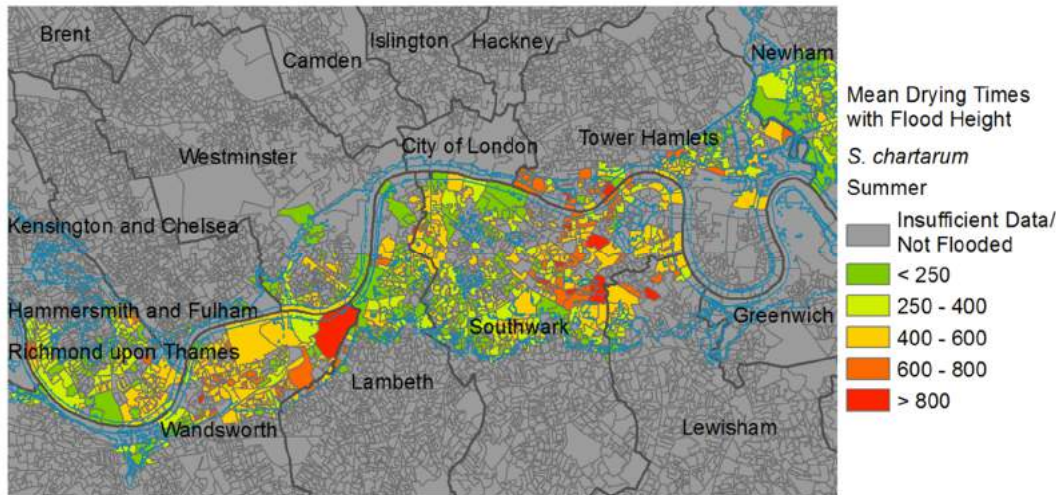
7
 8 **Figure 9. Average duration of risk (days) of contamination for *A. versicolor* following a winter flood.**



10
 11 **Figure 10. Average duration of risk (days) of contamination for *A. versicolor* following a summer flood.**
 12



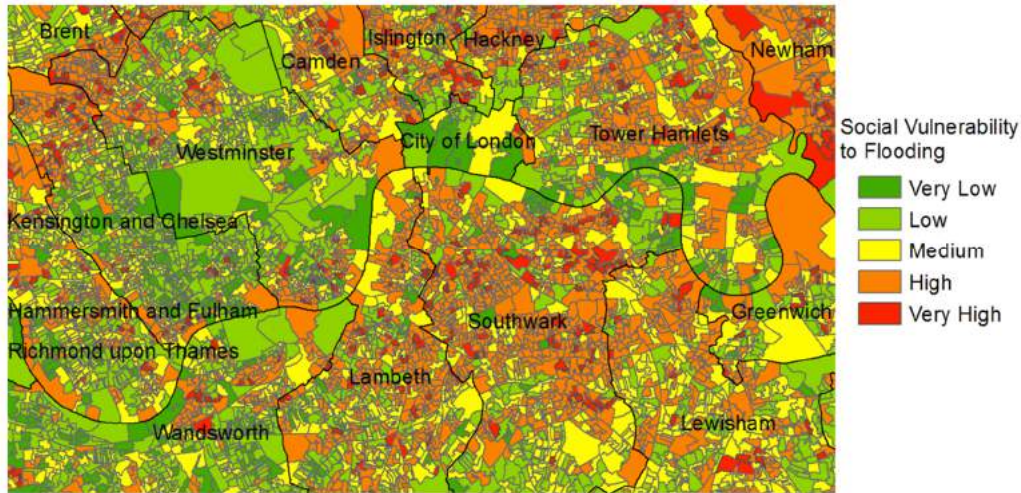
1
2
3 **Figure 11. Average duration of risk (days) of contamination for *S. chartarum* following a winter flood.**



4
5
6
7 **Figure 12. Average duration of risk (days) of contamination for *S. chartarum* following a summer flood.**

8 **3.2.3 Human Impact**

9
10 The social vulnerability to flooding analysis identified the more vulnerable populations that
11 live within London based on socio-economic data. The results of the SFVI analysis, generated
12 using the procedures explained in Tapsell et al (2002) can be seen in Figure 12. The social
13 vulnerability of Londoners to flooding increased towards the East of the research area, and
14 was particularly high in the London boroughs of Newham, and close to the river in
15 Southwark.
16

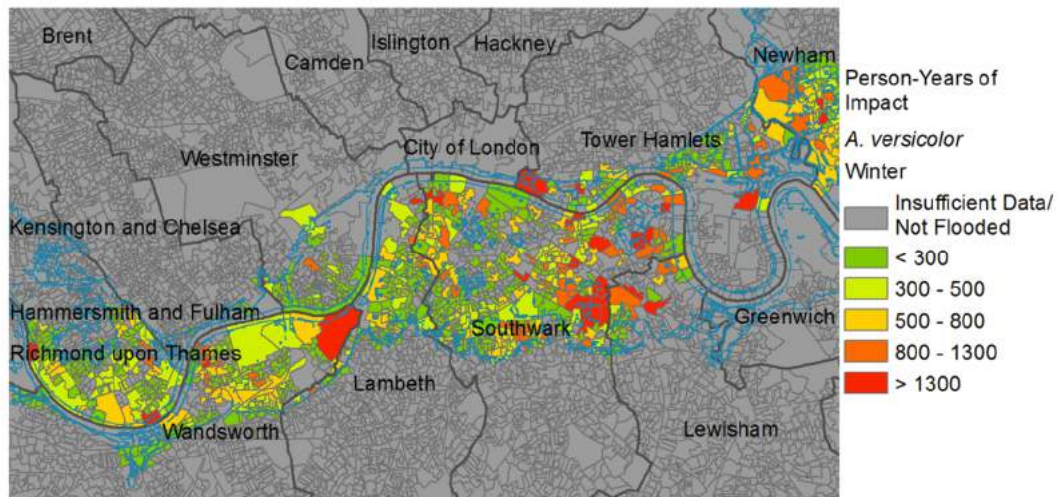


1
2 **Figure 13. Social vulnerability of populations in London to flooding based on the SFVI.**

3
4 Combining GIS Census data and flood maps indicated that a large of population of Londoners
5 would be affected by the 1-in-200 year tidal flood scenario. The number of domestic
6 buildings flooded, the estimated population affected, and the number of person-months that
7 the population would be impacted due to the drying behaviours of the buildings for each
8 Local Authority can be seen in Table 3. Southwark and Hammersmith and Fulham are likely
9 to experience the highest coverage of floodwater for the 1-in-200 year tidal flood, the greatest
10 number of flooded dwellings, and total flooded population. The largest impact in terms of
11 person-months was observed in the Borough of Southwark. An example of the calculated
12 person-years affected by the flood event can be seen in Figure 14.

13
14 **Table 3. Impact of a 1-in-200 year tidal flood event. Person-years are representative only, and are**
15 **extrapolated from buildings of known archetype only. Where there were no known archetypes**
16 **within a borough no person-years are reported.**

Local Authority	Estimated Population Flooded	Domestic Buildings Flooded		Total Person-Years			
		Total	Of which are known & modelled	<i>A. versicolor</i>		<i>S. chartarum</i>	
				Winter Flood	Summer Flood	Winter Flood	Summer Flood
City of London	18	17	0	-	-	-	-
Greenwich	5095	2506	0	-	-	-	-
Hammersmith and Fulham	40877	19465	4555	11947	51055	61421	42435
Kensington and Chelsea	1991	1082	32	84	2853	3073	1140
Lambeth	8831	4205	834	3523	17761	16776	9398
Lewisham	8332	3576	172	1116	23199	20532	12566
Newham	7477	3155	1648	6533	12507	13638	6782
Richmond upon Thames	160	80	0	-	-	-	-
Southwark	41645	18759	3477	19181	103484	95333	53318
Tower Hamlets	13440	6046	580	3744	39025	36555	17019
Wandsworth	15706	7841	3236	11187	27106	31587	19575
Westminster	5875	3363	166	611	12371	11981	5485
Total	149446	70095	14700	57925	289362	290895	167718



1
2 **Figure 14. Impact of the tidal 1-in-200 year flood event in terms of the potential displacement or**
3 **exposure to poor indoor conditions in person-years for *A. versicolor* following a winter flood.**
4

5 **4. Discussion**

6
7 By applying the building simulation results to the geospatial building stock data, areas of
8 London which are particularly vulnerable to flooding due to their combination of building
9 archetypes, flood risk, and sociodemographic profile have been identified.
10

11 **4.1 Comparative Dwelling Drying Behaviour**

12
13 By comparing the drying time of buildings flooded to the same height and drying under the
14 same conditions, it was possible to demonstrate the drying performance of locations in
15 London based on the most commonly occurring building types within these areas. The mould
16 species analysed showed a greater potential for long-term contamination in flooded dwellings
17 in the East of the research area, alongside the Thames. The London Borough of Southwark
18 was found to be particularly vulnerable to long-term mould growth following flooding.
19

20 This information can help identify locations vulnerable to a flood event, without modelling a
21 specific flooding scenario, and is relevant to insurance organisations, remediation
22 organisations, and government officials responsible for disaster response. While the maps are
23 for specific microbial species following a flood, the drying behaviours mapped can be
24 generalised to inform to potential for contamination of a range of moisture-dependent flood-
25 borne contaminants.
26

27 **4.2 Dwelling Drying Behaviour for Specific Flood Events**

28
29 The predictions of vulnerable locations within the research area using depth-drying curves
30 and the 1-in-200 year tidal flooding scenario provided predictions consistent with the
31 comparative drying rate observations, with the East of the research area around the Thames
32 identified as being particularly vulnerable to mould contamination. The developed curves can
33 be applied to other flood depth models in the future for other specific flooding scenarios,
34 provided there is sufficient coverage of building stock data with known archetypes.
35

36 The depth drying curves developed from the simulation data are best-estimates based on the
37 simulation results, and are not absolute values. These curves can be applied to estimate the

1 drying duration for periods up to one year, and in some cases can be used to extrapolate the
2 drying time for longer periods when simulation results show some degree of decline in
3 contamination levels within the simulation period. The need to extrapolate certain simulations
4 (for example modern purpose-built flats with brick/AAC walls flooded to 2m) means that
5 there is a greater uncertainty associated with these fitted curves.

6
7 The curves are only valid for heights above 0.1m and below 2.0m. Attempts to fit curves
8 through 0 for unflooded properties produced unstable models, and so were not incorporated.
9 For all properties flooded above 0m, the assumption is that the floor would be made wet,
10 meaning that the total surface area of the flooded building would not differ significantly from
11 the 0.1m flood height (excluding only the surface area of the walls), meaning that this likely
12 offers a good estimate of the drying times of smaller floods.

13
14 The depth-damage curves modelled based on the simulation data are applicable to the
15 scenarios used in the building simulation - namely, a 24 hour flood with freshwater. In
16 mapping the response of the building stock to a specific flood event, a large-scale tidal flood
17 has been used to determine the water depth. The 1-in-200 year tidal flood was used rather
18 than any of the freshwater flooding scenarios, as it allowed for the demonstration of the
19 drying ability across a wide range of the London building stock due to the large extent of the
20 flood. Since tidal floods will contain salts, it is likely that drying will take longer than the
21 simulation results suggest. None the less, the maps produced provide an indication of the
22 comparative drying abilities of the different COAs following a flood. For floods over 24
23 hours in length, more water may be absorbed into the building fabric. For many of the
24 modelled cases (Solid 9" Brick Walls, Brick Cavity Walls, Concrete), the walls reach
25 capillary saturation within 24 hours and no further water is absorbed, meaning the additional
26 duration of the flood will not impact on the drying time. For walls containing AAC, the
27 longer duration will allow more water to move into the material. This will result in the
28 already slow-drying AAC and insulated AAC walls, taking even longer to dry since there is a
29 greater amount of water to remove from the fabric. Consequently, longer flood durations will
30 result in the already at-risk areas becoming more at risk while the low-risk areas will remain
31 the same.

32
33 The depth drying curves also assume that the ground floor is at the same height as the
34 surrounding terrain, meaning that basements and subfloors are not considered. It is difficult to
35 estimate the ground floor level of buildings relative to surrounding terrain without conducting
36 individual surveys of buildings within the research area, however, an EHCS analysis included
37 in the EA Contaminated Land Exposure Assessment (CLEA) model suggests that the rate of
38 basements within properties modelled in this study is low (0 - 7.8% depending on archetype)
39 [EA, 2005]. As building stock models improve, it may be possible to refine the model further
40 to account for basements.

41
42 The likelihood of a flood event occurring which matches the extent and depth predicted by
43 the risk models is low, as flood models predict areas at risk, but that may not necessarily
44 experience flooding. However, as flood risk models can identify vulnerable properties within
45 a location, depth-drying curves can be used to identify vulnerable properties similar to how
46 depth-damage curves can be used to predict the cost of damage to a specific property, given a
47 flood event. The curves may also be applied retrospectively to predict the instantaneous risk
48 inside properties which have been abandoned following a flood event, to provide information
49 to occupants and remediation staff entering these properties for the first time after a flood. It
50 is important to note that the simulations that form the basis for the comparative drying times
51 and the actual drying curves are based on models which do not consider the impact of salts,
52 flood duration, and variation in built form on the drying behaviour, meaning that these results
53 are illustrative rather than definitive.

54

1 **4.3 Social Vulnerability and Dwelling Drying Performance**

2
3 The results of the SFVI indicate that the most vulnerable populations live in Southwark,
4 Newham, and in the North West of the research area in Brent and Westminster. The SFVI has
5 been developed to determine the relative vulnerability of populations to health problems
6 following a flood event. There are a number of different potential health consequences
7 following flooding, including exposure to microorganisms and mental health issues caused by
8 the trauma of a flood event and potential displacement from homes [Taylor et al., 2011]. By
9 identifying areas where both populations are vulnerable to flooding and buildings are
10 susceptible to long-term damp and microbial contamination, it is possible to predict locations
11 that may have a substantially increased health risk to the resident population. This is
12 particularly relevant when considering health issues caused by long-term exposure to
13 contaminants in the indoor environment or the length of time that an inhabitant is displaced
14 from their property, which will both be related to the drying behaviour of their dwelling.

15
16 Previous research has indicated that the slowest-drying building archetypes were post-war
17 and modern purpose-built flats, which may be the types of properties occupied by more
18 socially vulnerable individuals [Taylor et al, 2012]. The type of property that an individual
19 occupies may be a factor in their vulnerability to long-term health problems following a flood
20 event, and deserves further research.

21
22 The SFVI applied was developed following research into different flood events across the
23 UK, and so is likely to offer reasonable insights into the behaviour of the London population.
24 However, the London population may differ from the research population for many of the
25 metrics used to calculate the SFVI index - for example, non-car owners will be more
26 prevalent in London than in other areas of the UK. The differences in the population statistics
27 and behaviour may mean that the models estimate a higher vulnerability across the research
28 area than may actually exist.

29 30 **4.4 Highly Vulnerable Areas**

31
32 Areas where the actual drying time and the exposed population was high resulted in high
33 person-years of exposure to damp dwellings or long-term displacement. The hardest affected
34 borough is Southwark, with Hammersmith and Fulham and Lambeth both showing high
35 numbers of person-years of impact following the 1-in-200 year flood event. Person-years
36 provides a simple indication of the level of exposure to either displacement or damp indoor
37 conditions, and further analysis by epidemiologists may help to better understand the health
38 consequences across the research area. The person-years calculated may also help plan the
39 disaster response by providing an indication of the numbers and duration of alternative
40 accommodation necessary to prevent inhabitants remaining in unfit homes.

41
42 There were a number of locations where the vulnerability of the local building stock
43 coincided with locations that were at flood risk and where the population was vulnerable.
44 Wards such as Livesey, Rotherhithe, and South Bermondsey were vulnerable for multiple
45 reasons, and so should be given priority during long-term flood response planning. This may
46 include taking additional measures to ensure that the local population is provided with
47 alternative accommodation rapidly, and that mental health services are made available rapidly
48 to those affected by a flood event. Highly vulnerable properties include those built and
49 administered by local authorities as low-income housing. The information produced by this
50 research will enable local authorities to better plan the recovery and remediation of council-
51 owned flats in order to prevent major health problems among residents.

4.5 Limitations of Research

Both the comparative drying predictions and the depth drying curves make assumptions about the built form and wall type within the properties, which may not provide a precise estimate of the contaminant load and drying time within specific properties in relation to variations in building geometry and fabric. The built forms for the different age groups have been modelled so as to offer the drying behaviour of the worst-case scenario wall types - for example it has been observed that solid-closed cell (e.g. polyurethane) insulated cavity walls dry faster than glass fibre-insulated walls [Escarameia et al., 2007]. There was no data made available to this research on the rates of different types of insulation in cavity walls in the UK, and so by using the results for glass fibre rather than solid insulation, the model is able to account for one of the worst performing insulation types possible in flooded dwellings.

There were limits to the amount of building stock data available across the research area, and the areal information was estimated only from the numbers of known building types within the areal units. The amount of data available was also limited by the presence of unmodelled built form/age combinations and buildings that had not been identified in the CR database. Rather than make further assumptions about the characteristics of these properties, these were ignored in the spatial mapping of the vulnerability of areas of London. Further research can develop drying data for different buildings; meanwhile improvement of building stock models can help to reduce the numbers of unknown properties.

Building archetypes are meant to represent 'typical' buildings within a building stock, and as such are not representative of any individual property within the stock. The ecological fallacy is a misinterpretation of statistical data arising from the assumption that individual members of a population have the average characteristics of the population as a whole. The values presented in the areal units represent the drying time and vulnerability levels to flooding of all the buildings within this area, and it would be an ecological fallacy to conclude that these values apply to any individual unit within the area. The value of any individual property would be better estimated using the drying curves derived from the simulations.

By using the modal wall built forms and wall types within the COAs to estimate the comparative drying time, the results provide an indication of the majority built form, age, and wall type combination within the area. This ignores the variation of the building stock within the areal units, which is unlikely to be consistently of the same type, but is not vulnerable to skewing from properties that take an extended period to dry. The average dwelling time was calculated when mapping the actual drying time using the depth-damage curves. The number of known and modelled properties within a COA will influence the uncertainty of the estimate of the drying times for both modal and average calculations, and can be improved on as building stock information becomes more complete. The modelled information on the drying characteristics of different dwellings can also be improved by developing models for different building archetypes, archetypes with minority wall types, and those drying under different scenarios; however, the amount of time required to perform a simulation was prohibitively large, meaning it was unrealistic to simulate curves for all possible combinations of building, age, building envelope, and drying scenario within the limits of this research.

In mapping, the Modifiable Areal Unit Problem (MAUP) occurs when point-based phenomena is aggregated into areas. The areal values are heavily influenced by the 'modifiable' boundaries of the areas which can, in the UK for example, be reported in terms of COAs, Postcode Areas, Medium Level Census Output Areas, Local Authorities, Boroughs, and so on. By adjusting the boundaries, the areal value can change, and the interpretation of the map can change. By calculating areal statistics based on individual properties within areal units, the MAUP needs to be recognised. COAs were used as boundaries since they are the smallest units available with census and HEED data and because of the very local variations

1 in building stock and flood depths. Using larger areal units may change the conclusions of
2 the study, as the differences between areas may average out.

3
4 Despite the assumptions and limitations of the research, the results present a most useful
5 prediction of the vulnerability of the London domestic building stock to flooding, and when
6 combined with other flood-risk factors a useful picture of the potential chronic problems
7 following a flood event can be obtained.
8

9 **5. Conclusions**

10
11 Application of the simulation results to the GIS-based building stock data has revealed areas
12 of London where the building stock will be particularly prone to long-term contamination risk
13 following flooding. Many of these areas at risk of prolonged contamination also lie in areas at
14 risk of flooding, where the population may be more dense or vulnerable, or where there may
15 be the potential for elevated contamination in the water. In particular, the London Borough of
16 Southwark is predicted to be at particular risk following a large flood event due to the
17 combination of building types, flood risk and depth, social vulnerability, and population
18 density. Understanding these vulnerable locations can help to plan the response of the health
19 authorities, emergency services, remediation organisations, and local authorities to a flood
20 event. While the immediate response to flooding will depend on those hit hardest at the time
21 of the flood, the long-term response should consider the vulnerability of the population and
22 the buildings they inhabit in order to best manage the allocation of health resources, the
23 remediation of properties, and the provision of temporary accommodation for victims.

24 **7. Acknowledgements**

25 This research was carried out with funding from the EPSRC grant reference EP/G029881/1.
26 The author acknowledges the assistance of the Intrawise project in producing this work.
27

28 **8. References**

- 29
30
31 Blades, N., Biddulph, P., Cassar, M., Tuffnell, L. 2004. Modelling of climate change effects
32 on historic buildings. UCL Centre for Sustainable Heritage, London, UK.
33 Clarke, J.A., Johnstone, C.M., Kelly, N.J., McLean, R.C., Anderson, J.A., Rowan, N.J.,
34 Smith, J.E. 1998. A technique for the prediction of the conditions leading to mould growth in
35 buildings. *Build. Environ.* 34(4), 515-521.
36 DCLG. 2008. English Housing Survey. Department for Communities and Local Government.
37 London, UK.
38 Dumon, H., Palot, A., Charpin-Kadouch, C., Quéralt, J., Lehtihet, K., Garans, M., Charpin,
39 D. 2009. Mold species identified in flooded dwellings. *Aerobiologia.* 25(4), 341-344.
40 EnergyPlus. 2008. Getting started with EnergyPlus. US Department of Energy, Berkeley CA.
41 EA. 2005. Review of building parameters for development of a soil vapour intrusion model.
42 Environment Agency, Bristol, UK.
43 EA. 2010. Am I at risk of flooding? Environment Agency. Webpage.
44 <http://www.environment-agency.gov.uk/homeandleisure/floods/31650.aspx>. Accessed April
45 2nd 2011.
46 Escarameia, M., Karanxha, A., Tagg, A. 2007. Quantifying the flood resilience properties of
47 walls in typical UK dwellings. *Build. Serv. Eng. Res. Technol.* 28(3), 249-263.
48 EU. 2007. Global Climate Change Impact on Built Heritage and Cultural Landscapes.
49 European Union, Brussels, Belgium.

1 GLA. 2009. Climate Change Adaptaion Strategy. Greater London Authority, London, UK.
2 HEED. 2009. Homes Energy Efficiency Database. London, UK.
3 Hokoi, S., Kumaran, M.K. 1993. Experimental and analytical investigations of simulataneous
4 heat and moisture transport through glass fibre insulation. *J.Therm. Insul.Build. Envelopes.*
5 16, 263-292.
6 Hopkins, A., Lekov, A., Lutz, J., Rosenquist, G., Gu, L. 2011. Simulating a nationally
7 representative housing sample using EnergyPlus. Ernest Orlando Lawrence Berkeley National
8 Laboratory, US.
9 Hull City Council. 2009. Two years on - 2009. Hull, UK.
10 IBP. 2007. WUFI-2D. PC Program. Fraunhofer, Germany.
11 Nicolai, A., Grunewald, J. 2006. Delphin. PC Program. Dresden, Germany.
12 ONS (Office for National Statistics), 2001 Census: Standard Area Statistics (England and
13 Wales) [computer file]. ESRC/JISC Census Programme, Census Dissemination Unit, Mimas,
14 University of Manchester, UK.
15 OS. 2010. OS MasterMap Topography Layer. Ordnance Survey, Southhampton, UK.
16 Penning-Rowsell, E., Johnson, C., Tunstall, S., Tapsell, S., Morris, J., Chatterton, J., Green,
17 C. 2005. The benefits of flood and coastal risk management: a manual of assessment
18 techniques. Middlesex University Press, London, UK.
19 Priestnall, G., Jaafar, J., Duncan, A. 2000. Extracting urban features from LiDAR digital
20 surface models. *Computers.* 24, 65-78.
21 Solomon, G. M., Hjelmroos-Koski, M., Rotkin-Ellman, M., Hammond, S. K. 2006. Airborne
22 Mold and Endotoxin Concentrations in New Orleans, Louisiana, after Flooding, October
23 through November 2005, *Environ. Health Perspect.* 114(9), 1381-1386.
24 Tapsell, S. M., Tunstall, S. M. 2008. "I wish I'd never heard of Banbury": The relationship
25 between place and the health impacts from flooding. *Health & Place.* 14(2), 133-154.
26 Taylor, J., Lai, K.-M., Davies, M., Clifton, D., Ridley, I., Biddulph, P. 2011. Flood
27 management: prediction of microbial contamination in large-scale floods in urban
28 environments. *Environ. Int.*, 37(5), 1019-1029.
29 Taylor, J., Biddulph, P., Davies, M., Ridley, I., Mavrogianni, A., Oikonomou, E., Lai, K-M.
30 2012. Using building simulation to model the drying of flooded building archetypes. *J. .*
31 *Build. Perform. Simula.*, In Press
32 The Geoinformation Group. 2010. Cities Revealed: Leaders in aerial photos and GIS data.
33 Cambridge, UK.
34 ZunZun.com. Online data modelling. Webpage. www.zunzun.com. Accessed December 1st,
35 2011.
36
37